Study of hadronic J/ψ decays involving ϕ and ω production

A. Falvard, Z. Ajaltouni, H. Jnad, J. Jousset, B. Michel, and J. C. Montret
Laboratoire de Physique Corpusculaire, Université de Clermont II, F-63177 Aubière, France

R. Baldini, A. Calcaterra, and G. Capon
Laboratori Nazionali di Frascati dell'Istituto Nazionale di Física Nucleare, CP 13, I-00044 Frascati, Italy

J. E. Augustin, G. Cosme, F. Couchot, F. Fulda, G. Grosdidier, B. Jean-Marie, V. Lepeltier, F. Mane, and G. Szklarz
Laboratoire de l'Accélérateur Linéaire, Université de Paris-Sud, F-91405 Orsay, France

D. Bisello, G. Busetto, L. Pescara, P. Sartori, and L. Stanco
Dipartimento di Fisica dell'Università di Padova, e Istituto Nazionale di Física Nucleare, Sezione di Padova, I-35131 Padova, Italy
(DM2 Collaboration)
(Received 6 May 1988)

Hadronic decays of the J/ψ involving ϕ and ω production are investigated: $J/\psi\to\phi\pi^+\pi^-$, ϕK^+K^-, $\phi K_S^0K_S^0$, ωK^+K^-, $\omega K_S^0K_S^0$, $\phi K^*\bar{K}$, $\phi p\bar{p}$. Except $\phi K^*\bar{K}$ and $\phi p\bar{p}$, these three-body final states are dominated by quasi-two-body productions. A detailed study of the $f_0(975)$ production is presented. The analysis shows evidence for the $f_2(1720)$ being associated to both ω and ϕ. An upper limit is given for the $\phi\eta(1440)$ branching ratio.

I. INTRODUCTION

The *radiative* J/ψ decays whose inclusive branching ratio accounts for about 8% of the J/ψ decays are expected to be a good place to observe gluonia production through the classical diagram in Fig. 1. These decays have been investigated by the Crystal Ball, Mark II, and Mark III Collaborations at the SLAC storage ring SPEAR and by the DM2 Collaboration at the DCI storage ring. The most significant results of these experiments remain the discovery and analysis of the $\eta(1440)$ and $f_2(1720)$ states; moreover very interesting structures have been recently observed in γ-vector-vector final states.[1,2]

Unfortunately, the mechanism depicted in Fig. 1 does not provide an unambiguous signature for glue bound-state production. For instance, radiative production of standard pseudoscalars η, η' and tensors $f_2(1270)$, $f_2'(1525)$ is well understood[3] by the coupling of their SU(3)-singlet component to the two-gluon system. So, it is important to get information from other J/ψ channels or from different production reactions, in order to clarify the nature of these glueball candidates.

Actually, about 80% of the J/ψ decays are purely hadronic final states and it has been proposed long ago[4] to use this pure initial state to perform refined hadronic spectroscopy including glueball search.

Since the J/ψ decays mainly to hadrons via a multigluon intermediate state, three-body mesonic states as $J/\psi\to VPP$ (V=vector; P=pseudoscalar) can be produced through the sequential process[5] described in Fig. 2(a) and named connected diagram. Disconnected diagrams [for instance, Fig. 2(b)] are found to contribute at the predicted level[6] of 10% of the $q\bar{q}$ production amplitude in the decays $J/\psi\to$vector+pseudoscalar.[7] The dominance of connected diagram to produce $q\bar{q}$ mesons seems also to be valid for classical tensor mesons since:[8] $B(J/\psi\to\omega f_2'(1525))\ll B(J/\psi\to\omega f_2(1270))$, as expected assuming $f_2(1270)$ and $f_2'(1525)$ mesons to be quasi-ideally mixed tensors. More precise results are presented in this paper. On the contrary, gluonic mesons as $f_2(1720)$ could be strongly produced through disconnected diagrams.

Finally, different authors[9,10] proposed to use the $J/\psi\to\phi\pi\pi$ decay to look also for a narrow 0^{++} glueball below 1 GeV/c^2 decaying into $\pi\pi$.

This paper presents the improved measurements by the DM2 experiment on the search for $J/\psi\to\phi f_2(1720)$, $\omega f_2(1720)$ in the channels $J/\psi\to\phi\pi^+\pi^-,\phi K\bar{K},\omega K\bar{K}$. The $J/\psi\to\omega\pi\pi$ decay, which benefits from a very large statistics will be treated in a separate paper. The observation, in connection to the previous analysis, of J/ψ decays into $\phi 4\pi^{\pm}$, $\phi K_S^0K^{\pm}\pi^{\mp}$ (including $\phi K^*\bar{K}$), $\phi p\bar{p}$ is reported.

After a description of the DM2 detector (Sec. II), Secs. III–VI present the various inclusive three-body decays. Sections VII–X deal with the observed quasi-two-body

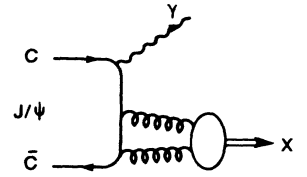

FIG. 1. Diagram for radiative decay of the J/ψ.

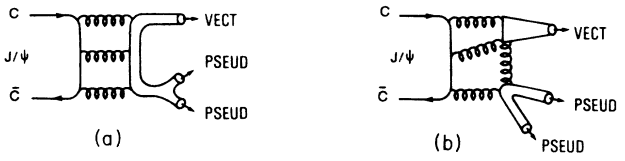

FIG. 2. Diagram for hadronic decays of the J/ψ: (a) connected diagram and (b) disconnected diagram.

dynamics. All the results are obtained from $(8.6\pm1.3)\times10^6$ J/ψ produced with the e^+e^- Orsay storage rings DCI.

II. THE DM2 DETECTOR

The DM2 is a solenoidal detector with large acceptance which measures charged-particle momenta and both photon directions and energies. A layer of scintillators inside the coil is used for triggering and for particle identification. The apparatus is described in detail in Ref. 11 and only acceptances and an update of subdetector resolutions are given in Table I. The photon energy measurement is not used in the following analysis, the events being well constrained by the photon direction measurements alone.

III. $J/\psi\to\phi\pi^+\pi^-,\phi K^+K^-,\phi p\bar{p}$

The ϕ is observed in its K^+K^- decay mode. The studied channels are searched for among four charged-track events with total charge and vertex inside a fiducial volume. The missing momentum must be lower than 80 MeV/c to reject most of the events with π^0's or γ's in the final state.

A. ϕ selection

The ϕ is selected in the following by imposing.

(i) The time of flight (TOF) of both particles, when measured, must be consistent with kaon hypothesis, within 3σ.

(ii) At least one K^+K^- mass combination must satisfy $|M_{K^+K^-}-M_\phi|\leq0.010$ GeV/c^2. In less than 10% of the events, two combinations satisfy this constraint. In the search for $J/\psi\to\phi K^+K^-$, the combination with a mass closest to the nominal ϕ mass is retained. For the other channels, the one which gives the best χ^2 in the kinematical four constraint (4C) fit (Sec. III C) is selected.

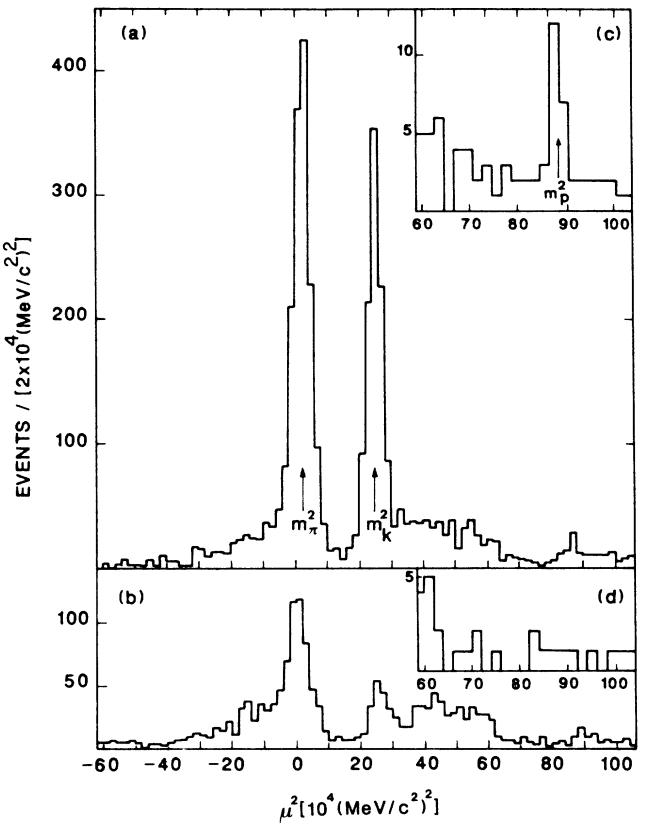

FIG. 3. Square mass of $X^\pm$ charged particles produced against the ϕ for the candidates $J/\psi\to\phi X^+X^-$: (a) in ϕ band, (b) in ϕ sidebands, (c) proton region ϕ band, and (d) proton region sidebands.

TABLE I. Characteristics of the DM2 detector. MWPC stands for multiwire proportional chamber.

Subdetector	Acceptance	Resolutions
Internal detector (2 MWPC + 13 drift chambers)	87% 4π	Momentum: 3.5% at 1 GeV/c
Time of flight (36 scintillators)	80% 4π	540 ps dominated by beam spread (440 ps)
Photon detector: (barrel) (8 octants; $5X_0$; lead–scintillator–streamer-tubes sandwiches)	70% 4π	Photon energy: $\frac{19\%}{\sqrt{E}}$ for $E\leq300$ MeV; 35% for $E\geq300$ MeV. Photon directions: 10 mrad in azimuth, 7 mrad in polar angle
Photon detector: (end caps) ($5X_0$; lead-MWPC sandwiches)	12% 4π	20 mrad in azimuth and polar angle

The background is estimated from the ϕ sidebands, defined by

$$0.020 \leq | M_{K^+K^-} - M_\phi | \leq 0.040 \text{ GeV}/c^2 .$$

B. Kinematics

Assuming that the two particles of momenta p_+ and p_- recoiling against the ϕ have the same mass μ, one can derive, from the energy-momentum conservation law,

$$\mu^2 = \frac{(E^2 - p_+^2 - p_-^2)^2}{4E^2} \quad \text{with } E = M_{J/\psi} - E_\phi .$$

Figures 3(a) and 3(b) show the histogram of this variable for events in the ϕ band and ϕ sidebands, respectively. Large signals around $\mu^2 = m_\pi^2$ and m_K^2 in Fig. 3(a) show evidence for $J/\psi \to \phi\pi^+\pi^-$ and $J/\psi \to \phi K^+K^-$ decays whereas only a hint of a $J/\psi \to \phi p\bar{p}$ signal is visible.

C. $J/\psi \to \phi\pi^+\pi^-$

Figures 4(a) and 4(b) show the μ^2 distribution after the TOF cut.[12] The Monte Carlo simulation indicates that the $J/\psi \to \phi\pi^+\pi^-$ events contribute weakly to ϕ sidebands (3%). So, the peak around $\mu^2 = M_\pi^2$ in Fig. 4(b) is mostly induced by $J/\psi \to K^+K^-\pi^+\pi^-$ without ϕ dynamics. The contamination from $J/\psi \to K_S^0 K^\pm \pi^\mp$ is found to be completely negligible.

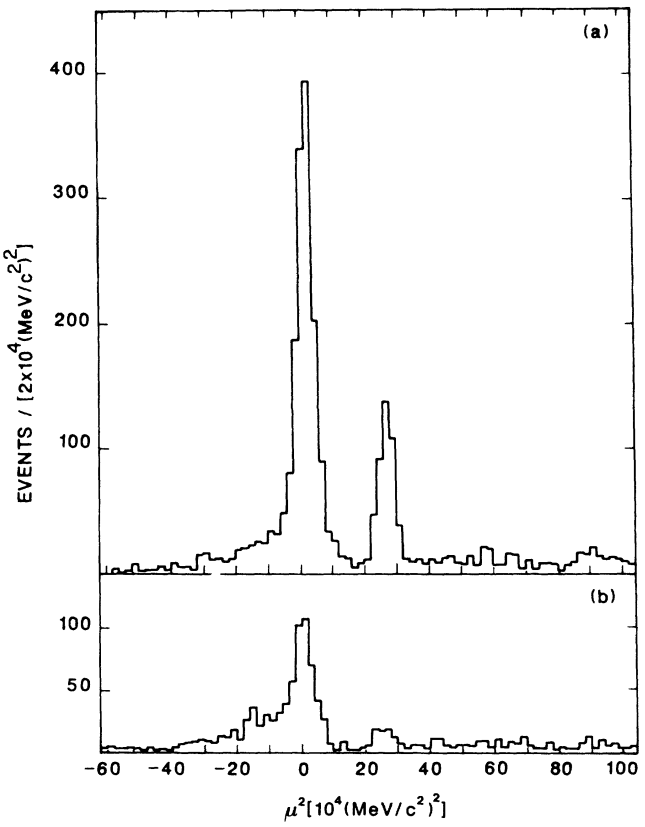

FIG. 4. Square mass after TOF imposed on $X^\pm$ particles against the ϕ: (a) $X = \pi$ in ϕ band and (b) $X = \pi$ in ϕ sideband.

The events in the band $|\mu^2 - M_\pi^2| \leq 5 \times 10^4$ (MeV/c^2)^2 are then 4C fit to improve the resolution on the $\pi^+\pi^-$ invariant mass. The resulting spectrum is shown in Fig. 5. The total number of background events is obtained from the events of Fig. 4(b) in the $|\mu^2 - M_\pi^2| \leq 5 \times 10^4$ (MeV/c^2)^2 mass region and by normalizing ϕ band and ϕ sidebands in the squared mass region $-30 \times 10^4 \leq \mu^2 \leq -10 \times 10^4$ (MeV/c^2)^2 where no $J/\psi \to \phi X^+X^-$ decay can contribute.

Using the efficiency curve shown in Fig. 5(c) (Ref. 13), the following branching ratio is measured:

$$B(J/\psi \to \phi\pi^+\pi^-) = (7.8 \pm 0.3 \pm 1.2) \times 10^{-4} .$$

The structures observed in Fig. 5(a) will be discussed in Secs. VII–IX.

D. $J/\psi \to \phi K^+K^-$

The μ^2 spectrum of the remaining events, after the TOF cut, is given in Figs. 6(a) and 6(b). The ϕK^+K^- contribution is enhanced.

The events observed in ϕ sidebands at $\mu^2 = M_K^2$ [Fig. 6(b)] amounts to about 10% of the signal present in ϕ band [Fig. 6(a)]. The Monte Carlo simulation indicates that it is almost saturated by the combinatorial background of the $J/\psi \to \phi K^+K^-$ decay itself. The events are then 4C fit. The K^+K^- invariant-mass distribution is shown in Fig. 7 for the events in the range $|\mu^2 - M_K^2| \leq 6 \times 10^4$ (MeV/c^2)^2. With the efficiency of Fig. 7(c), one gets

$$B(J/\psi \to \phi K^+K^-) = (8.3 \pm 0.3 \pm 1.3) \times 10^{-4} .$$

The structures observed in Fig. 6(a) will also be discussed in Secs. VII–IX.

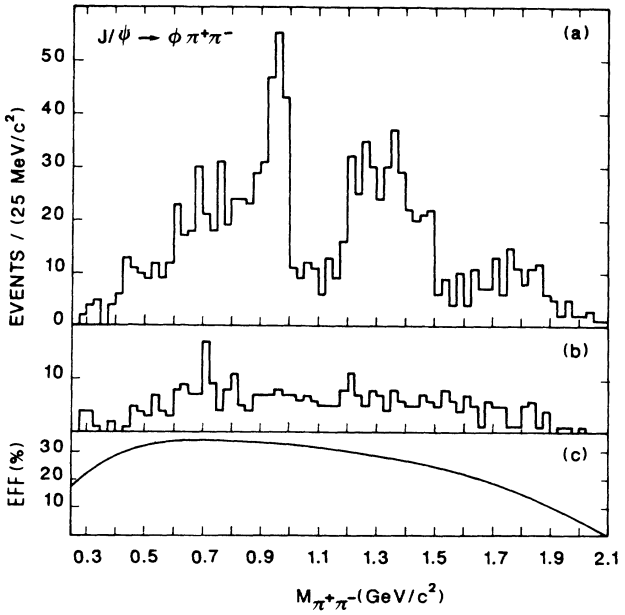

FIG. 5. $\pi^+\pi^-$ invariant mass in $J/\psi \to \phi\pi^+\pi^-$: (a) ϕ band, (b) ϕ sidebands, and (c) efficiency.

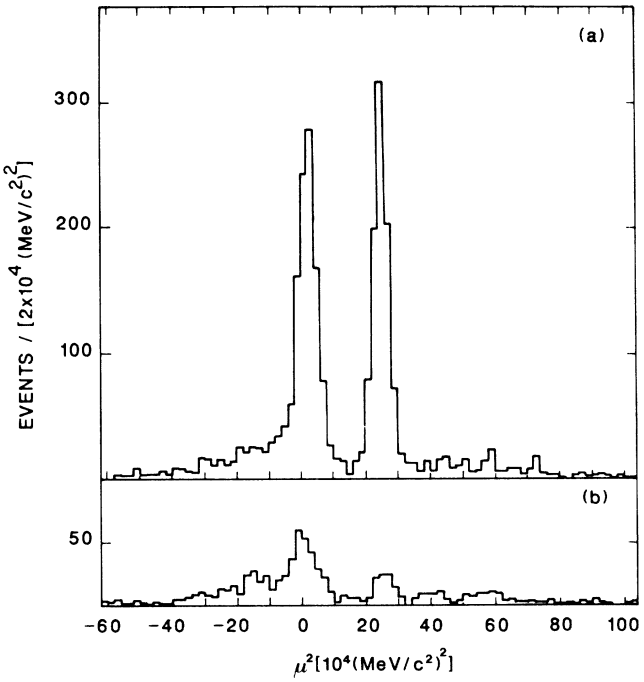

FIG. 6. Square mass after TOF imposed on $X^{\pm}$ particles against the ϕ: (a) $X=K$ in ϕ band and (b) $X=K$ in ϕ sideband.

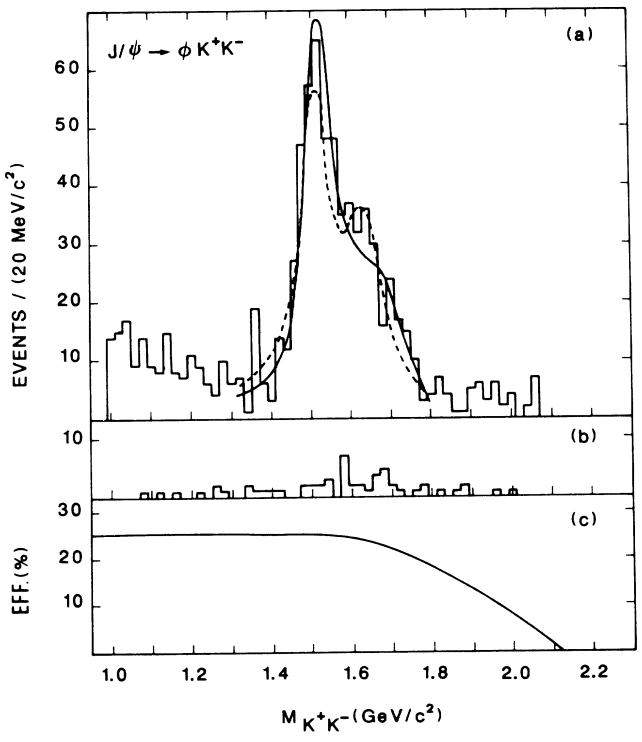

FIG. 7. K^+K^- invariant mass in $J/\psi\to\phi K^+K^-$: (a) ϕ band, (b) ϕ sidebands, and (c) efficiency. The solid line in (a) is the fit described in Sec. VII including $f_2(1525)$ and $X(1700)$ interference. The dotted line is the result of the fit without interference.

E. $J/\psi\to\phi p\bar{p}$

By requiring that the TOF of both particles recoiling against the ϕ be consistent with a proton hypothesis, (17 ± 5) events are observed in a peak [Figs. 3(c) and 3(d)] having mass and width consistent with the values expected for $J/\psi\to\phi p\bar{p}$. This signal corresponds to

$$B(J/\psi\to\phi p\bar{p})=(4.5\pm1.3\pm0.7)\times10^{-5}\ .$$

This value is very small compared to the branching ratio for the decay $J/\psi\to\omega p\bar{p}$ (Ref. 14): $(78\pm15)\times10^{-5}$. This effect is mainly explained by the reduction of phase space and by the Okubo-Zweig-Iizuka (OZI) rule which reduces the production of a color-singlet $s\bar{s}$ pair associated to $p\bar{p}$.

IV. $J/\psi\to\phi2(\pi^+\pi^-),\phi K_S^0K_S^0,\phi K_S^0K^{\pm}\pi^{\mp}$

These channels are analyzed in the $K^+K^-2(\pi^+\pi^-)$ or $K^+K^-(\pi^+\pi^-)(K^{\pm}\pi^{\mp})$ final states. Events with six charged tracks and zero total charge are selected. The tracks are not constrained to belong to a common vertex. The missing momentum must be smaller than 120 MeV/c.

The total energy distribution of these events when all the particles are assumed to be pions (Fig. 8) shows large contributions from $J/\psi\to6\pi^{\pm},K_S^0K^{\pm}\pi^{\mp}\pi^+\pi^-$, $K^+K^-4\pi^{\pm}$ and a large bump below 2.3 GeV which is dominated by baryonic productions $\Xi^*\bar{\Xi}^*$, $\Sigma^*\bar{\Sigma}^*$, etc.

The ϕ signal is evident in the K^+K^- invariant-mass distribution (Fig. 9) obtained from the particles consistent with a TOF kaon assignment. In the following, the ϕ is selected as in Sec. III A whereas the ϕ sidebands are defined by $0.020\le|M_{K^+K^-}-M_{\phi}|\le0.030$ GeV/c^2.

Finally, the TOF cut is applied on the four remaining particles.

A. $J/\psi\to\phi4\pi^{\pm}$

The total energy is shown in Figs. 10(a) and 10(b) for the selected events in ϕ band and ϕ sidebands, respectively. A large $J/\psi\to\phi4\pi^{\pm}$ signal is prominent in Fig. 10(a).

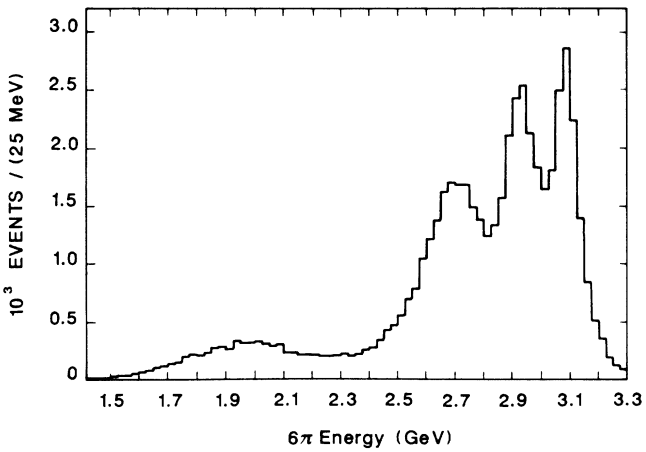

FIG. 8. Total energy for $J/\psi\to6$ *charged particles* assuming all particles are π.

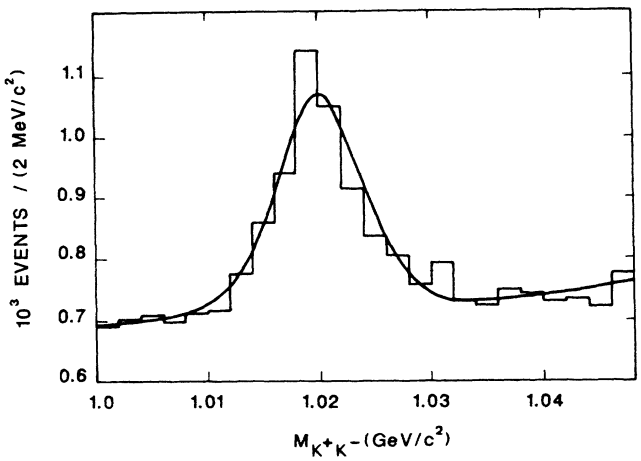

FIG. 9. K^+K^- invariant mass for all $J/\psi \to 6$ charged events with the ϕ signal.

A large fraction of the small peak in ϕ sidebands at the J/ψ mass is combinatorially produced by the decay itself, as the Monte Carlo simulation predicts,

$$\frac{N(\phi 4\pi)_{\rm sb}}{N(\phi 4\pi)_{\phi \rm b}} = 17\% ,$$

where $N(\phi 4\pi)_{\rm sb}$ and $N(\phi 4\pi)_{\phi \rm b}$ denote the number of events predicted in the sidebands and ϕ band, respectively. The $J/\psi \to K^+K^-\pi^+\pi^-\pi^+\pi^-$ decay without ϕ dynamics also contributes to the J/ψ peak in Fig. 10 since its branching ratio is large as visible in Fig. 8.

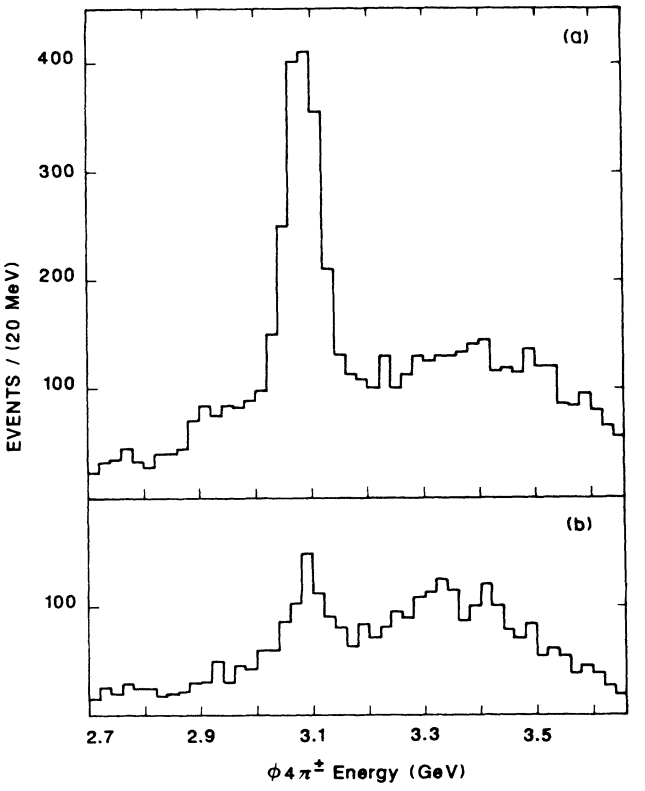

FIG. 10. $\phi 4\pi$ total energy: (a) ϕ bands and (b) ϕ sidebands.

After background subtraction taking into account the previous remarks (1335±42) events are found in the energy range

$$|E_{K^+K^-2(\pi^+\pi^-)} - M_{J/\psi}| \leq 0.070 \text{ GeV} .$$

The 4π invariant-mass spectrum after a 4C fit is displayed in Fig. 11. Assuming that the $\phi 4\pi$ events are distributed according to phase space (solid curve), the following branching ratio is calculated:

$$B(J/\psi \to \phi 4\pi^{\pm}) = (1.6 \pm 0.1 \pm 0.3) \times 10^{-3} .$$

B. $J/\psi \to \phi K_S^0 K_S^0$

Figures 12(a) and 12(b) give the scatter plot of the $\pi^+\pi^-$ invariant-mass combinations for the events with $|E_{K^+K^-2(\pi^+\pi^-)} - M_{J/\psi}| \leq 0.070$ GeV in Figs. 10(a) and 10(b), respectively. They show the $K_S^0K_S^0$ signal associated with the ϕ. To isolate this production, both $\pi^+\pi^-$ masses are required to lie within the range [0.465, 0.525] GeV/c^2. Figure 13 shows the total energy of the events in Fig. 10(a) selected by the last cut and gives evidence of the $J/\psi \to \phi K_S^0 K_S^0$ signal.

The $K_S^0K_S^0$ invariant-mass spectrum in ϕ band and ϕ sidebands after selecting the total energy within the range [3016,3176] MeV is presented in Figs. 14(a) and 14(b), respectively. The overplotted curve in Fig. 14(a) is explained in Sec. IX. The measured branching ratio

$$B(J/\psi \to \phi K^0 \bar{K}^0) = (6.3 \pm 0.7 \pm 1.6) \times 10^{-4}$$

agrees with the value obtained for $J/\psi \to \phi K^+K^-$ in Sec. III D.

C. $J/\psi \to \phi K_S^0 K^{\pm}\pi^{\mp}, \phi(K^*\bar{K}+\text{c.c.})$

For this channel, a K_S^0 is selected among the four tracks in front of the ϕ by the cut (Fig. 15)

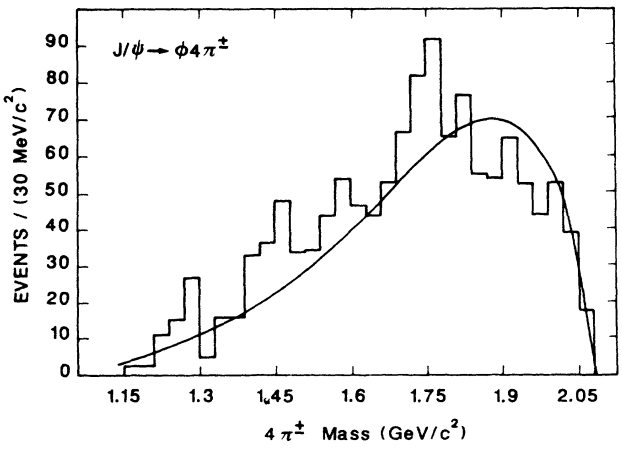

FIG. 11. 4π invariant mass in $J/\psi \to \phi 4\pi$ (background subtracted). The curve is the shape of phase-space distribution.

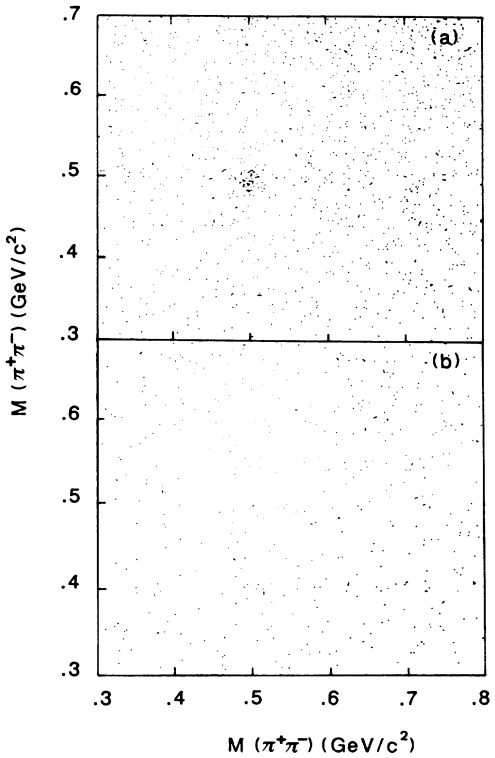

FIG. 12. $\pi^+\pi^-$ scatter plot in $J/\psi\to\phi 4\pi$: (a) ϕ band (b) ϕ sidebands.

$$|M_{\pi^+\pi^-}-M_{K_S^0}|\leq 0.030\ \text{GeV}/c^2\ .$$

The remaining two particles have to be one pion and one kaon and are identified, whenever possible, according to their TOF. Thus, Figs. 16(a) and 16(b) show the total energy with $\phi K_S^0 K^+\pi^-$ or $\phi K_S^0 K^-\pi^+$ correct hypotheses. The $J/\psi\to\phi K_S^0 K^\pm\pi^\mp$ signal is observed in Fig. 16(a) together with a residual $\phi 4\pi$ contribution. It should be noticed that the $J/\psi\to\phi K_S^0 K^\pm\pi^\mp$ Monte Carlo simulation reproduces the small enhancement at the J/ψ mass in the

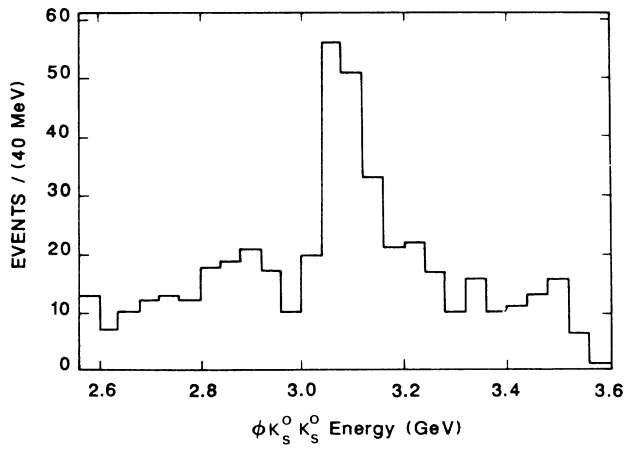

FIG. 13. ($2K4\pi$) energy for $\phi K_S^0 K_S^0$ candidates. The peak around 3.1 GeV evidences the $J/\psi\to\phi K_S^0 K_S^0$ decay.

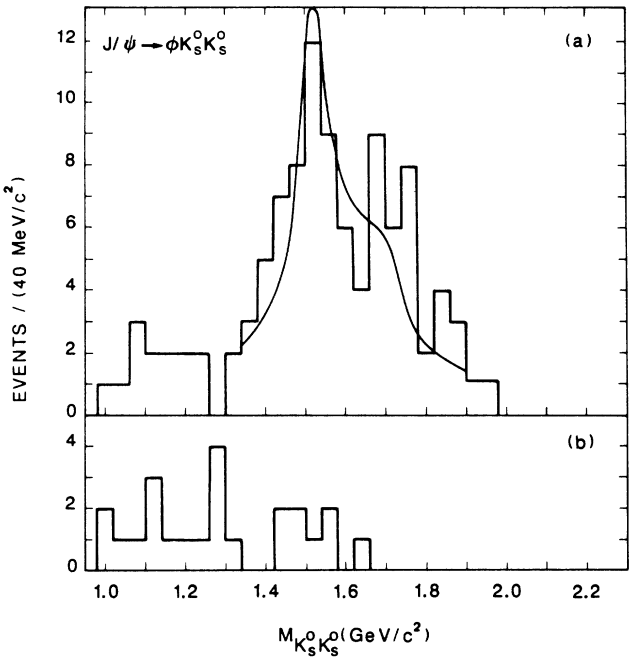

FIG. 14. $K_S^0 K_S^0$ mass for $J/\psi\to\phi K_S^0 K_S^0$: (a) ϕ band, the curve is the expectation from ϕK^+K^- and (b) ϕ sidebands.

ϕ sidebands [Fig. 16(b)]. A cut is applied on the total energy

$$|E_{\phi K_S^0 K^\pm\pi^\mp}-M_{J/\psi}|\leq 0.050\ \text{GeV}\ .$$

About 90% of the accepted events have only one correct combination of the six charged tracks assignment.

From the measured events, the following branching ratio is obtained:

$$B(J/\psi\to\phi K_S^0 K^\pm\pi^\mp)=(7.4\pm 0.9\pm 1.1)\times 10^{-4}\ .$$

The $K_S^0 K^\pm\pi^\mp$ invariant mass is shown in Figs. 17(a) and 17(b). No signal is observed within the $\eta(1440)$ mass

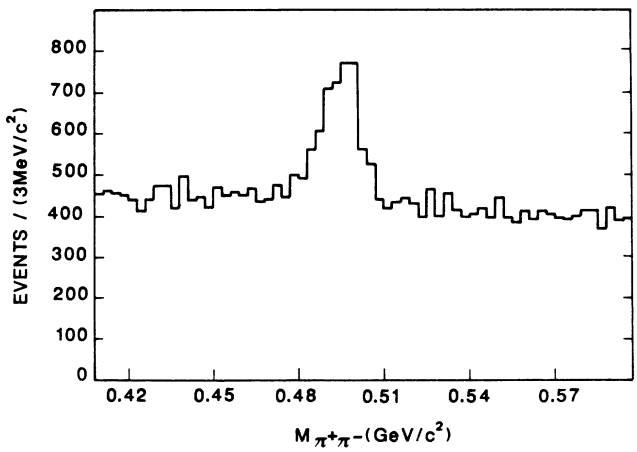

FIG. 15. $\pi^+\pi^-$ invariant mass in front of ϕK_S^0.

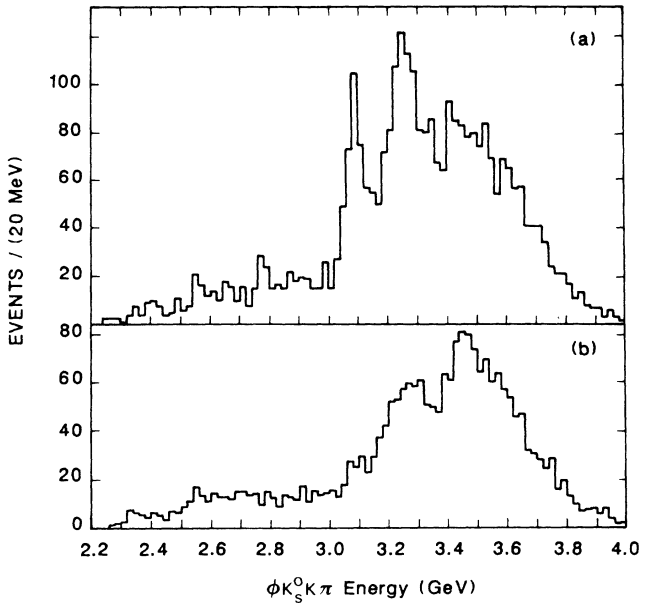

FIG. 16. $\phi K_S^0 K^{\pm}\pi^{\mp}$ energy: (a) ϕ band and (b) ϕ sidebands.

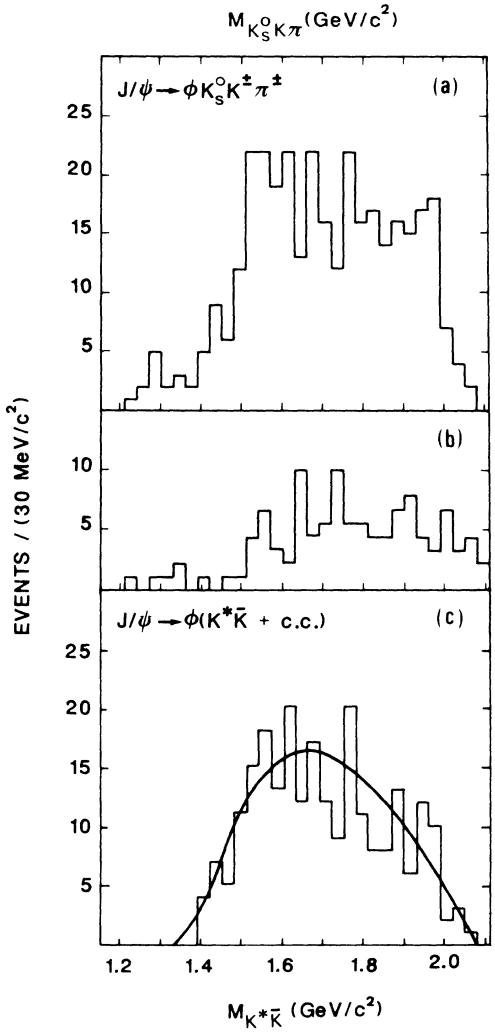

FIG. 17. $K_S^0 K^{\pm}\pi^{\mp}$ invariant mass for $J/\psi \to \phi K_S^0 K^{\pm}\pi^{\mp}$ candidates. (a) ϕ band; (b) ϕ sidebands; and (c) $K^*\bar{K}$ invariant mass. The curve is the prediction for phase space.

range. This translates to

$$B(J/\psi \to \phi\eta(1440)) \times B(\eta(1440) \to K\bar{K}\pi) < 2.5 \times 10^{-4} (90\%\ \text{C.L.}) .$$

Then $K_S^0\pi^{\pm}$ and ($K^+\pi^-$ or/and $K^-\pi^+$) invariant mass are computed for each event and shown in Fig. 18. A large K^* signal is evidenced. Selecting the K^* signal by the cut

$$| M_{K\pi} - M_{K^*} | \leq 0.060\ \text{GeV}/c^2$$

and assuming three-body phase-space distribution [Fig. 17(c)], the following branching ratio is obtained:

$$B(J/\psi \to \phi(K^*\bar{K} + \text{c.c.})) \times B(K^*\bar{K} \to K_S^0 K^{\pm}\pi^{\mp}) = (6.9 \pm 0.8 \pm 1.0) \times 10^{-4} .$$

This value agrees with the recent result of Mark III (Ref. 15) for $J/\psi \to \phi K^*\bar{K} \to \phi K\bar{K}\pi$.

V. $J/\psi \to \omega K^+ K^-$

The ω is observed in its $\pi^+\pi^-\pi^0$ decay mode. Thus, the four charged-track events with zero total charge and a common vertex are used to analyze this channel. Since these events have to be selected in the presence of a large background, the observation of the two photons from π^0 decay is required.

These events are 2C fit to the $\pi^+\pi^- K^+ K^- \gamma\gamma$ hypothesis ($\chi^2 < 8$). The events from the residual $J/\psi \to 2\pi^+ 2\pi^- \pi^0$ background are totally rejected if $\chi^2_{5\pi} < 20$ when fitted to this hypothesis. A background from $J/\psi \to K_S^0 K^{\pm}\pi^{\mp}\pi^0$ decay is still present. In fact, a clear K_S^0 contribution is seen in the sample of remaining events (Fig. 19). In order to eliminate this background,

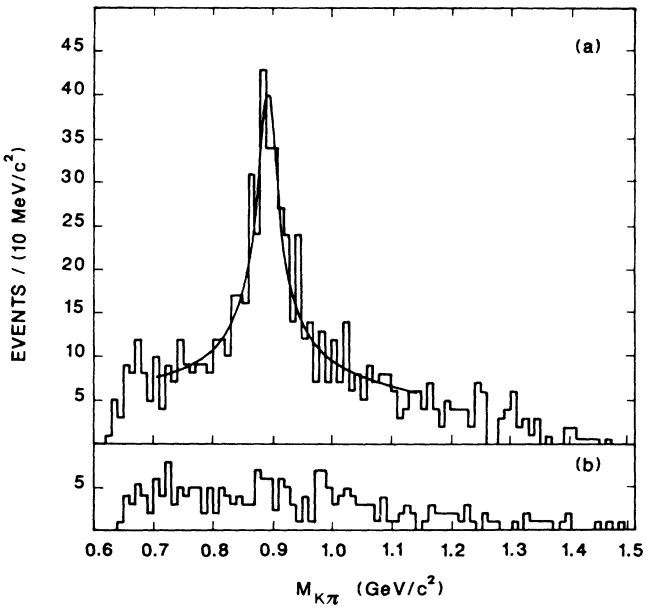

FIG. 18. $K\pi$ mass for $J/\psi \to \phi K_S^0 K^{\pm}\pi^{\mp}$ candidates: (a) ϕ band, the curve is the fit with standard K^* parameters and (b) ϕ sidebands.

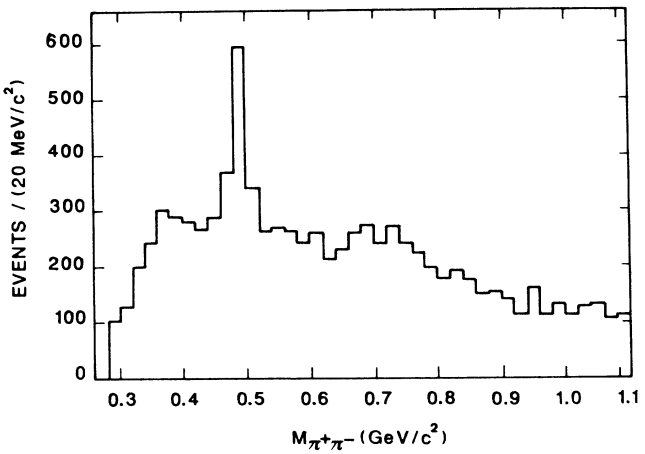

FIG. 19. $\pi^+\pi^-$ invariant mass.

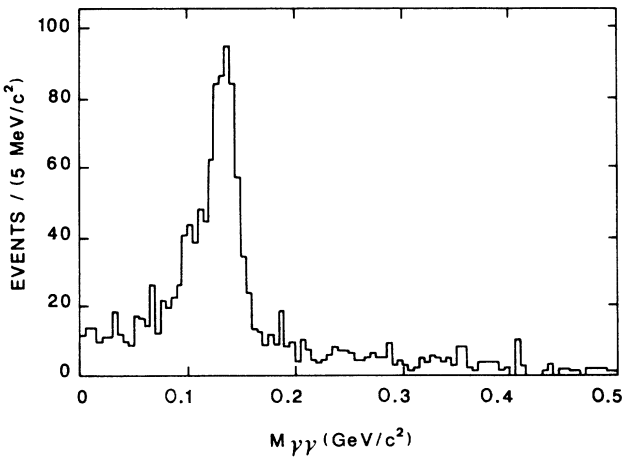

FIG. 21. $\gamma\gamma$ invariant mass.

the following cut is applied:

$$|M_{\pi^+\pi^-}-M_{K_S^0}|>0.030 \text{ GeV}/c^2 .$$

Figure 20 shows the $\pi^+\pi^-\pi^0$ mass distribution after selecting a π^0 by a cut on the 2γ mass (Fig. 21): $|m_{\gamma\gamma}-M_{\pi^0}|\leq 0.035$ GeV/c^2 and applying the TOF cut. The ω signal[16] is seen and selected by

$$|M_{\pi^+\pi^-\pi^0}-M_\omega|<0.040 \text{ GeV}/c^2 .$$

The K^+K^- mass in front of the ω is shown in Fig. 22. The structure around 1.7 GeV/c^2 will be discussed in Sec. IX. After subtracting the background determined from ω sidebands ($80\leq|M_{\pi^+\pi^-\pi^0}-M_\omega|\leq 160$ MeV/c^2), one gets

$$B(J/\psi\rightarrow\omega K^+K^-)=(7.4\pm0.7\pm2.3)\times10^{-4} .$$

VI. $J/\psi\rightarrow\omega K_S^0K_S^0$

Both K_S^0 are observed in their $\pi^+\pi^-$ decay mode. The total energy of six charged-track events assuming a missing π^0 is required to range between 2.9 and 3.3 GeV and γ's from the π^0 decay have to be detected.

The $\pi^+\pi^-\pi^0$ mass distribution (Fig. 23) shows the ω signal from $J/\psi\rightarrow\omega4(\pi^\pm)$. The $J/\psi\rightarrow\omega K_S^0K_S^0$ channel is selected by the following requirements: At least one $K_S^0\rightarrow\pi_1^+\pi_1^-$ secondary vertex with $|M_{K_S^0}-M_{\pi^+\pi^-}|\leq 30$ MeV/c^2; at least one mass of the two remaining $\pi^+\pi^-$ pairs and the π^0 must satisfy the ω cut defined as

$$|M_{\pi_2^+\pi_2^-\pi^0}-M_\omega|\leq 0.075 \text{ GeV}/c^2$$

and ω sidebands are defined by

$$0.075\leq|M_{\pi_2^+\pi_2^-\pi^0}-M_\omega|\leq 0.200 \text{ GeV}/c^2 .$$

Figures 24(a) and 24(b) show the invariant mass of the

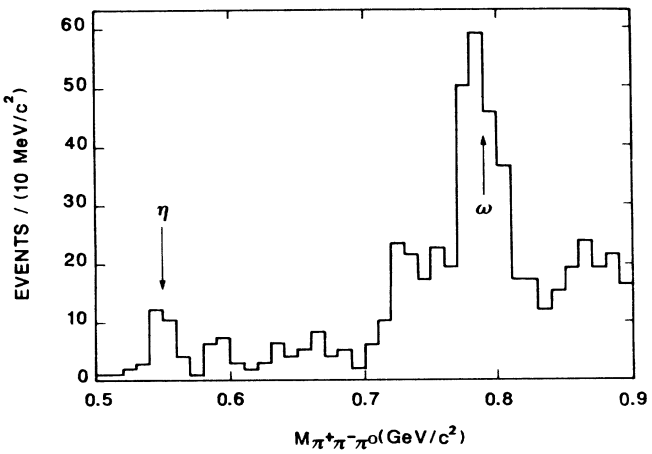

FIG. 20. $\pi^+\pi^-\pi^0$ invariant mass for $J/\psi\rightarrow3\pi K^+K^-$ candidates.

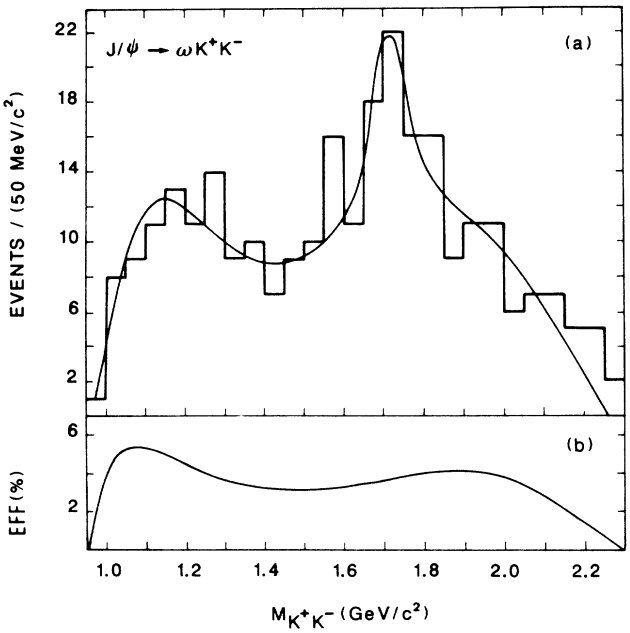

FIG. 22. (a) K^+K^- invariant mass against the ω for $J/\psi\rightarrow\omega K^+K^-$ candidates; the curve is a fit described in the text (Sec. IX) and (b) efficiency.

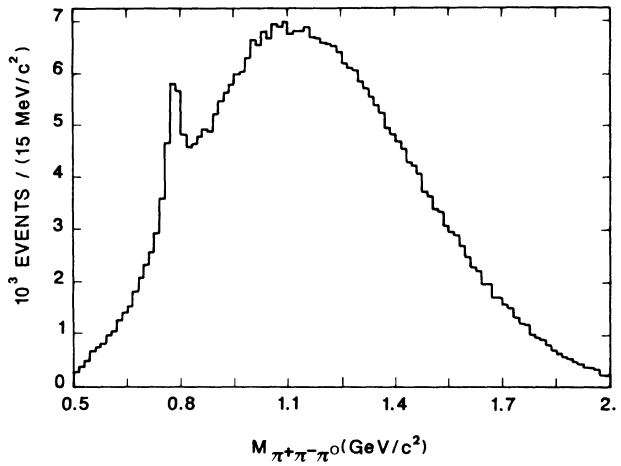

FIG. 23. $\pi^+\pi^-\pi^0$ invariant mass for $J/\psi\to 7\pi$ candidates.

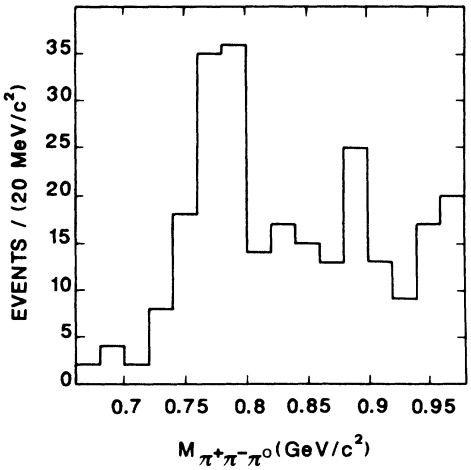

FIG. 25. $\pi^+\pi^-\pi^0$ invariant mass for $J/\psi\to\pi^+\pi^-\pi^0K_S^0K_S^0$ candidates.

last $\pi_3^+\pi_3^-$ pion pair when the $\pi_2^+\pi_2^-\pi^0$ mass lies in the ω band and in ω sidebands, respectively. A large peak is found at the K_S^0 mass. The Monte Carlo simulation indicates that the small peak at the K_S^0 mass observed in the ω sidebands is not induced by the decay $J/\psi\to\omega K_S^0K_S^0$. This peak could be due to the $J/\psi\to\pi^+\pi^-\pi^0K_S^0K_S^0$ decay without ω dynamics.

After selecting the second K_S^0 in the mass range [0.472,0.522] GeV/c^2, Fig. 25 shows the ω signal. From Fig. 24 one concludes that (80±13) events are produced from $J/\psi\to\omega K_S^0K_S^0$ corresponding to

$$B(J/\psi\to\omega K^0\bar{K}^0)=(12.4\pm2.0\pm3.1)\times10^{-4}\ .$$

This value agrees with the one measured for $J/\psi\to\omega K^+K^-$ (Sec. V). Figure 26 shows the $K_S^0K_S^0$ invariant-mass spectra in ω band and ω sidebands, respectively. An excess of events is found around 1.7 GeV/c^2 as observed for the decay $J/\psi\to\omega K^+K^-$.

VII. $f_0(975)$ PRODUCTION

The $\pi^+\pi^-$ mass spectrum in the $J/\psi\to\phi\pi^+\pi^-$ decay exhibits a clean and large $f_0(975)$ (formerly S^*) signal [Fig. 5(a)]. Its production can be interpreted by a sequential mechanism [Fig. 2(a)] and a large $s\bar{s}$ or $s\bar{s}(u\bar{u}+d\bar{d})/\sqrt{2}$ component in the $f_0(975)$. The steep fall on the high mass side of the $f_0(975)$ cannot be well reproduced by a Flatté distribution[17] [Fig. 27(a)]. Thus a

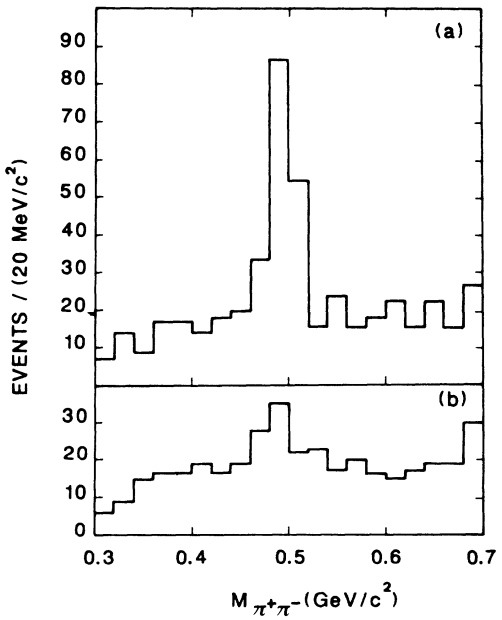

FIG. 24. $\pi^+\pi^-$ invariant mass in front of ωK_S^0: (a) ω band and (b) ω sidebands.

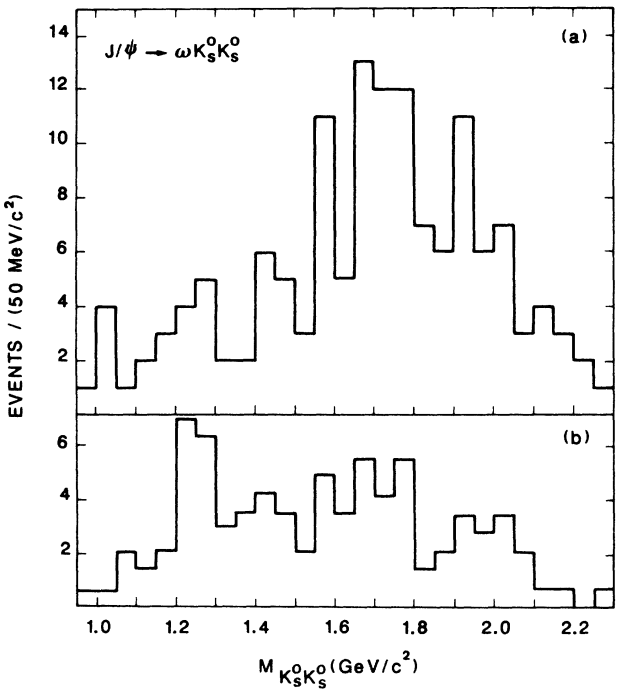

FIG. 26. $K_S^0K_S^0$ invariant mass for $J/\psi\to\omega K_S^0K_S^0$ candidates: (a) ω band and (b) normalized ω sidebands.

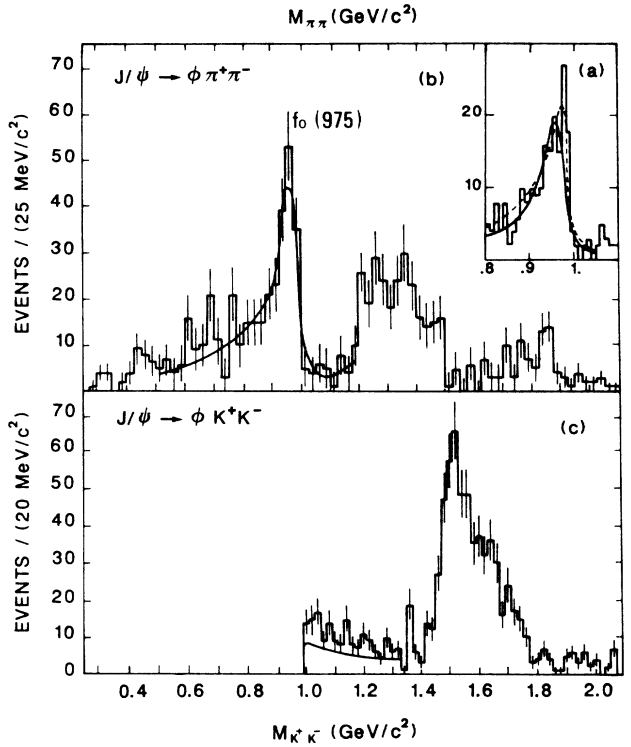

FIG. 27. (a) Fit of the $f_0(975)$ signal by a Flatté distribution (solid line); the dotted line is the shape of the fit described in Sec. VII A. (b) $\pi^+\pi^-$ invariant-mass distribution for $J/\psi\to\phi\pi^+\pi^-$ after background subtraction. The fit is described in the text. (c) K^+K^- invariant-mass distribution from $J/\psi\to\phi K^+K^-$. The curve is the $f_0(975)$ contribution as calculated in Sec. VII B.

fit of the $\pi^+\pi^-$ spectrum below 1 GeV/c^2 needs a correct description of the $K\bar{K}$ threshold. The model proposed by Mennessier[18] has been used in the following.

A. Fitting the $\pi\pi$ mass spectrum in $J/\psi\to\phi\pi\pi$

In this model, the $\pi^+\pi^-$ invariant-mass distribution in the process $J/\psi\to\phi\pi^+\pi^-$ is computed by adding the direct couplings (Fig. 28) of the J/ψ to the $\phi\epsilon$ and ϕS^* final states (ϵ and S^* are the bare scalar isoscalar fields used in Ref. 18 to describe the S-wave $\pi\pi$ interaction):

$$|A_{\pi^+\pi^-}|^2=\tfrac{2}{3}|e_{J/\psi}e_\phi(f_\epsilon T_{\epsilon\pi}+f_{S^*}T_{S^*\pi})|^2,$$

where $e_{J/\psi}$ and e_ϕ are, respectively, the polarizations of the J/ψ and ϕ, f_ϵ and f_{S^*} the coupling constants of the J/ψ to the $\phi\epsilon$ and ϕS^* final states, and $T_{\epsilon\pi}$ and $T_{S^*\pi}$ the $\epsilon\to\pi\pi$ and $S^*\to\pi\pi$ amplitudes. Let us note that the term $e_{J/\psi}e_\phi$ in the amplitude is valid only in the case where the (ϕ,ϵ) and (ϕ,S^*) systems are produced in relative S wave. This hypothesis is consistent with the angular distribution of the ϕ (Fig. 29). The best fit of the data after background subtraction [Fig. 27(b)] is obtained for

$$\frac{f_{S^*}}{f_\epsilon}=-2.53\ .$$

FIG. 28. Definition of f_e and f_{S^*}.

Notice that the steep fall around 1 GeV/c^2 is accounted for by the interference between $f_\epsilon T_{\epsilon\pi}$ and $f_{S^*}T_{S^*\pi}$. In this formalism, one gets

$$B(J/\psi\to\phi f_0(975))B(f_0(975)\to\pi^+\pi^-)$$
$$=(2.4\pm0.2\pm0.4)\times10^{-4}\ .$$

At last, the angular distribution of the π^+ versus the $f_0(975)$ direction in the f_0 rest frame supports a spin-0 assignment [Fig. 30(a)].

B. Fitting the K^+K^- threshold in $J/\psi\to\phi K^+K^-$

The fit of the $\pi^+\pi^-$ mass spectrum gives in this model an absolute prediction for the ϕK^+K^- mode near threshold with

$$|A_{K^+K^-}|^2=\tfrac{1}{2}|e_{J/\psi}e_\phi(f_\epsilon T_{\epsilon K}+f_{S^*}T_{S^*K})|^2,$$

f_ϵ and f_{S^*} being taken from the fit of the $\pi^+\pi^-$ spectrum. Figure 27(c) shows the K^+K^- production at a threshold from this coupled-channel analysis.

The good agreement observed does not exclude other small contributions near the $K\bar{K}$ threshold. For instance, a theoretical approach was recently proposed[19] to compute the nonresonant pseudoscalar-pseudoscalar (PP) continuum produced in the OZI-allowed decays $J/\psi\to$vector PP. Applied to $J/\psi\to\omega\pi^+\pi^-$, it gives a

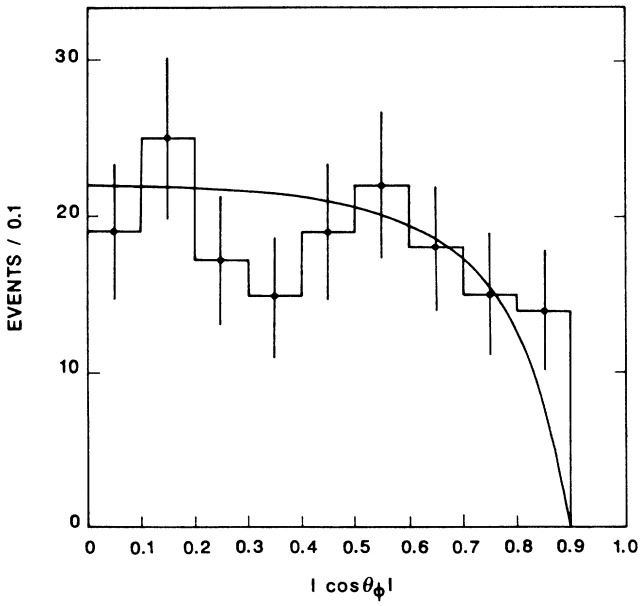

FIG. 29. ϕ angular distribution in $J/\psi\to\phi f_0(975)$. The curve is the prediction of S-wave production.

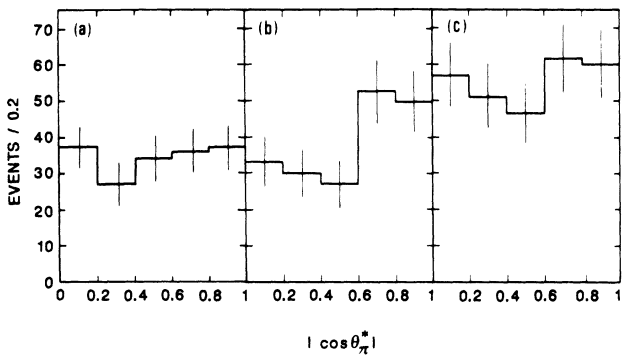

FIG. 30. π^+ angular distribution in the $\pi\pi$ rest frame. (a) $\cos\theta^*_\pi$ under the $f_0(975)$: the curve is the $f_0(975)$ 0^+, (b) $\cos\theta^*_\pi$ in the $\pi\pi$ mass range $1.2 \leq M_{\pi\pi} \leq 1.3$ GeV/c^2, and (c) $\cos\theta^*_\pi$ in the $\pi\pi$ mass range $1.3 \leq M_{\pi\pi} \leq 1.5$ GeV/c^2.

possible explanation of the large bump observed[20] at low $\pi\pi$ mass.

A recent attempt was made to interpret the $f_0(975)$ and $a_0(980)$ as $K\bar{K}$ molecule.[21] In this model, the ratio $B(J/\psi\to\phi f_0(975))/B(J/\psi\to\omega f_0(975))$ is equal to 2 (Ref. 22) (Fig. 31). The branching ratio of $J/\psi\to\omega f_0(975)$ is measured by the DM2 Collaboration:[2,23] tion:[2,23]

$$B(J/\psi\to\omega f_0(975))\times B(f_0(975)\to\pi^+\pi^-) = (1.10\pm0.21\pm0.16)\times10^{-4} .$$

Then

$$\frac{B(J/\psi\to\phi f_0(975))}{B(J/\psi\to\omega f_0(975))} = 2.2\pm0.5 ,$$

which does not conflict with the $K\bar{K}$ molecule prediction.

VIII. $J/\psi\to\phi f_2(1270),\phi f_0(1300)$

The mass distribution of the $\pi^+\pi^-$ system recoiling against the ϕ [Fig. 27(b)] shows a broad bump between 1.1 and 1.5 GeV/c^2 corresponding to

$$B(J/\psi\to\phi\pi^+\pi^-)_{1.1\leq M_{\pi\pi}\leq 1.5} = (2.5\pm0.2\pm0.4)\times10^{-4} .$$

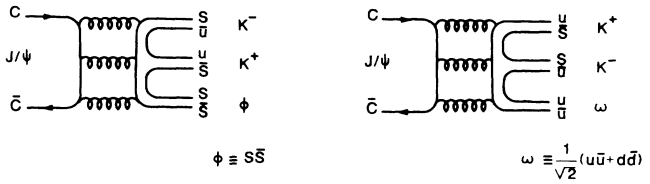

FIG. 31. Diagrams for $J/\psi\to\phi+(K\bar{K}$ molecule) and $J/\psi\to\omega+(K\bar{K}$ molecule).

The efficiency is shown in Fig. 5(c).

A single Breit-Wigner amplitude cannot fit properly to this bump. Its shape looks like the $\pi\pi$ S-wave structure observed in $\pi N\to\pi\pi N$ (Ref. 24) and associated to $f_0(1300)$ [formerly $\epsilon(1300)$] production.

The $J/\psi\to\phi f_2(1270)$ decay is expected to be small compared to $J/\psi\to\omega f_2(1270)$ if connected diagrams dominate. In fact there is no peak at the $f_2(1270)$ mass in Fig. 27(b).

Nevertheless the angular distribution of the π^+ in the $\pi\pi$ rest frame indicates a possible nonscalar contribution in the mass range $1.2 \leq M_{\pi^+\pi^-} \leq 1.3$ GeV/c^2 [Fig. 30(b)], while the high mass part of the bump is consistent with the decay of a spin-0 state [Fig. 30(c)]. A more sophisticated angular analysis is not possible due to the limited available statistics.

At last, let us notice that, from the measurement given in Sec. IX, only 10–20 events are expected to be produced by the $J/\psi\to\phi f_2'(1525)\to\phi\pi^+\pi^-$ decay.

A. $J/\psi\to\phi f_0(1300)$, limit on $J/\psi\to\phi f_2(1270)$

When fitting to two Breit-Wigner amplitudes added coherently or incoherently [one of them having the $f_2(1270)$ parameters], one gets very poor χ^2's. Results of both fits are given in Table II, and the dotted line in Fig. 33 below shows the coherent fit.

The most conservative way to conclude is to give an upper limit for the $\phi f_2(1270)$ decay assuming that the whole bump between 1.1 and 1.5 GeV/c^2 is produced by this channel. This leads to

$$B(J/\psi\to\phi f_2(1270)) < 4.5\times10^{-4} \quad (90\%\ \text{C.L.}) .$$

TABLE II. Fits of the bump observed in the $J/\psi\to\phi\pi^+\pi^-$ decay in the $M_{\pi\pi}$ range [1.1; 1.5] GeV/c^2.

Hypothesis	Mass and width of X (1.3)	$B(\phi f_2(1270))$ (10^4)	$B(\phi X(1.3)\to\phi\pi\pi)$ (10^4)	χ^2/DF
$f_2(1270)$ and $X(1300)$ without interference	1373±8 106±11	1.68±0.12±0.25	2.20±0.11±0.33	3.3
$f_2(1270)$ and $X(1300)$ with interference[a]	1443±16 140±23	4.3 ±0.18±0.65	2.17±0.11±0.33	2.8

[a]The fitted phase is about 180°.

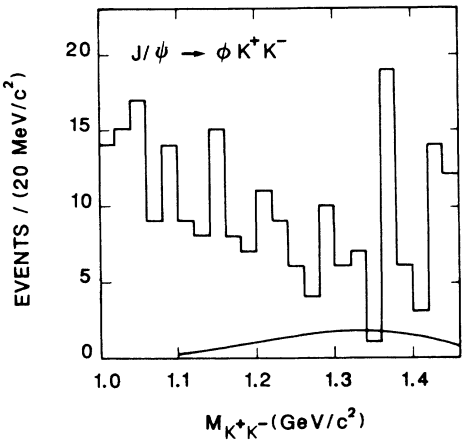

FIG. 32. K^+K^- mass in $J/\psi \to \phi K^+K^-$. The curve is the prediction for $J/\psi \to \phi f_0(1300) \to \phi K^+K^-$.

On the other hand, assuming the full bump between 1.1 and 1.5 GeV/c^2 to be induced by $f_0(1300)$ production and using the tabulated branching ratios of this state,[8] the corresponding signal in the decay $J/\psi \to \phi K^+K^-$ can be inferred. This prediction is compared to the data in Fig. 32.

B. Limit on tensor mixing angle

Assuming nonet symmetry in the $J/\psi \to$ vector + tensor decays, this limit on branching ratio can be converted into a limit on the tensor mixing angle θ_T. A SU(3) calculation including SU(3) breaking gives

$$\frac{A(\phi f_2(1270))}{A(\omega f_2(1270))} = \frac{1-\sqrt{2}t}{\sqrt{2}+t} \times \frac{g-2h-2xe}{g+e} ,$$

where $A(\phi f_2(1270))$ and $A(\omega f_2(1270))$ are the SU(3) amplitudes for both decays g,e,h,x are defined in Sec. IX D and $t=\tan(\theta_T)$.

Thus assuming the $J/\psi \to$ vector + tensor decays are dominated by S wave or D wave, and using the $J/\psi \to \omega f_2(1270)$ branching ratio given in Refs. 20 and 23, the following limits are obtained:

$$|\theta_T - 35.3°| \leq 29° \ (S \text{ wave}) ,$$

$$|\theta_T - 35.3°| \leq 33° \ (D \text{ wave}) \ (950003 \text{ C.L.})$$

(35.3° is the ideal mixing angle).

IX. $f_2'(1525)$ AND $f_2(1720)$ PRODUCTION

The naive assumption that glueballs should decay as an SU(3) singlet conflicts with a glueball assignment for the $f_2(1720)$ which is mainly observed in radiative J/ψ decays[25] in its $K\bar{K}$ mode.[26,27] Moreover, Cohen, Isgur, and Lipkin[28] indicated that this conclusion could be modified by large interference terms between the ground state and radially excited states. To obtain more information on the nature of the $f_2(1720)$, Senba and Tanimoto[29] proposed to look for $J/\psi \to \phi f_2(1720), \omega f_2(1720)$.

The K^+K^- mass spectra associated with the ϕ (Sec. III, Fig. 7) and the ω (Sec. V, Fig. 22) are quite different. The ω associated production shows a large bump $X(1700)$ around 1.7 GeV/c^2. On the contrary, the ϕ associated production is dominated by a large $f_2'(1525)$ contribution with a clear shoulder on its high mass side.

A. Search for $J/\psi \to \phi f_2(1720)$

By assuming first that the shoulder in Fig. 7 is attributed to the $X(1700)$, identified with $f_2(1720)$, two fits have been done. As $f_2'(1525)$ and $f_2(1720)$ are $J^{PC}=2^{++}$ particles, their production amplitudes have been assumed to interfere. In the first fit (Table III) the masses and widths are left free for both particles; in the second case, we impose the mass and width of the $f_2'(1525)$. This reduces the fitted width of the $X(1700)$ and, consequently, its branching ratio. In both cases the mass and width of the $X(1700)$ are consistent with the parameters of the

TABLE III. Fits of the f_2' and of the shoulder observed at a higher mass in the $J/\psi \to \phi K^+K^-$ decay.

Hypothesis	f' and $X(1.7)$ free and interference	$X(1.7)$ free and interference	f' and $X(1.7)$ free without interference
Phase (rd)	3.19±0.06	3.21±0.09	
f' mass	1496±2	1515[a]	1515±5
f' width	100±3	85[a]	62±10
$X(1.7)$ mass	1690±4	1700±10	1638±10
$X(1.7)$ width	184±6	125±18	148±17
$B(J/\psi \to \phi f' \to \phi K^+K^-) \times 10^4$	5.0±0.2	4.4±0.2	2.8±0.1
$B(J/\psi \to \phi X(1.7) \to \phi K^+K^-) \times 10^4$	3.3±0.15	1.8±0.1	3.7±0.15
χ^2/DF	1.0	1.6	2.7

[a]Imposed: the f' mass and width are not the tabulated one; but they are not strongly fixed by previous experiments and the values have been chosen to give a correct fit of the left-hand side of the f'.

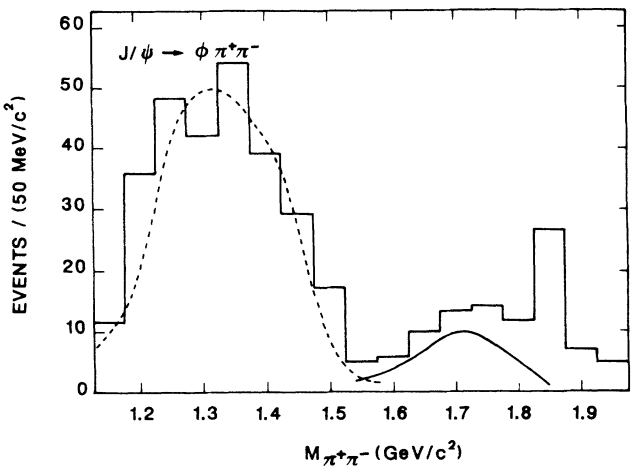

FIG. 33. $\pi^+\pi^-$ mass in $J/\psi\to\phi\pi^+\pi^-$. The solid line is the prediction for $J/\psi\to\phi f_2(1720)\to\phi\pi^+\pi^-$. The dotted line is the result of the second fit in Table II.

$f_2(1720)$ (Ref. 30) measured in radiative J/ψ decays.[26,27]

The K^+K^- invariant-mass spectrum has also been fitted to two Breit-Wigner amplitudes without interference (Table III). The $f_2'(1525)$ mass and width are found very close to their standard values and the mass of $X(1700)$ is significantly smaller than the standard value for $f_2(1720)$. These various fits are displayed in Fig. 7.

Using the results of the second fit in Table III the contribution of the $f_2'(1525)$ and $X(1700)$ in the $\phi K_S^0 K_S^0$ channel is computed. The result is presented by the curve in Fig. 14(a) which is an absolute prediction assuming isoscalar productions. The agreement between data and computation is good but the comparison suffers from low statistics of the $J/\psi\to\phi K_S^0 K_S^0$ channel.

Finally, assuming that the $X(1700)$ is the $f_2(1720)$ and using the result of fit 2 in Table III, (50±20) events[31] should be produced through $J/\psi\to\phi f_2(1720)$, $f_2(1720)\to\pi^+\pi^-$ in the $\pi\pi$ mass range [1.5,1.9] GeV/c^2. This is not in disagreement with the data (Fig. 33) which show an excess of events above 1.6 GeV/c^2. Here too, a more detailed analysis would require larger statistics.

B. Search for $J/\psi\to\omega f_2(1720)$

Analysis of the $J/\psi\to\omega K^+K^-, \omega K_S^0 K_S^0$ decay modes is presented in Secs. V and VI, respectively. In Fig. 22 the histogram is fitted to a Breit-Wigner amplitude added to a quadratic polynomial both being weighted by three-body phase-space and detector efficiency. The parameters obtained for $X(1700)$,

$$M=1716\pm21\ \text{MeV}/c^2,\quad \Gamma=129\pm39\ \text{MeV}/c^2,$$

are well consistent with the $f_2(1720)$ ones. One measures

$$B(J/\psi\to\omega X(1700))B(X(1700)\to K^+K^-)=(2.0\pm0.6\pm0.3)\times10^{-4}.$$

An enhancement in the same mass range is also observed in the $\omega K^0\bar{K}^0$ mode [Fig. 26(a)]. After background subtraction, the following branching ratio is obtained:

$$B(J/\psi\to\omega X(1700))B(X(1700)\to K^0\bar{K}^0)=(2.8\pm0.9)\times10^{-4},$$

the error being dominated by uncertainty on background subtraction.

No signal is observed in Fig. 22 for $\omega f_2'(1525)$ production; as for the nonobservation of $\phi f_2(1270)$, it is consistent with dominance of connected diagrams [Fig. 2(a)]. The following upper limit is set:

$$B(J/\psi\to\omega f_2'(1525))B(f_2'(1525)\to K\bar{K})<2\times10^{-4}\ \ (95\%\ \text{C.L.}).$$

C. Comments on hadronic production of $X(1700)$

The previous results support the identification of the observed $X(1700)$ with the $f_2(1720)$ although a spin-parity analysis would be necessary to firmly establish this hypothesis. If the $f_2(1720)$ is associated to the vector singlet part ω_0 as expected for a glueball candidate, the ratio of productions is predicted to be

$$|A(\phi f_2(1720))/A(\omega f_2(1720))|^2=\tfrac{1}{2}$$

up to a kinematical factor equal to p_V or p_V^5 if the process appears in the S wave or D wave, respectively. This naive calculation predicts that $B(J/\psi\to\phi f_2(1720))/B(J/\psi\to\omega f_2(1720))$ should range between 0.38 (S wave) and 0.14 (D wave). Using the result of fit 2 in Table III, only the S-wave hypothesis is marginally consistent with our measurement:

$$\frac{B(J/\psi\to\phi f_2(1720))}{B(J/\psi\to\omega f_2(1720))}=0.91\pm0.28.$$

But such an excess of $\phi f_2(1720)$ production could be due to a larger coupling of $f_2(1720)$ to strange quark as indicated by its small $\pi\pi$ vs $K\bar{K}$ decay width.

D. Comparison of $\phi f_2'(1525)$ production with other vector-tensor final states

$\phi f_2'(1525)$ production can be related to other vector + tensor J/ψ decays by SU(3) symmetry. In fact, assuming that $f_2(1270)$ and $f_2'(1525)$ are ideally mixed tensors, the amplitudes of $\phi f_2'(1525)$, ρA_2, and $\omega f_2(1270)$ final states are related, except for an additional kinematical factor, by the following expressions:

$$A(\omega f_2(1270))=g+e,$$

$$A(\rho^0 A_2^0)=A(\rho^+ A_2^-)=A(\rho^- A_2^+)=g+e,$$

$$A(\phi f_2'(1525))=g-2h-2xe,$$

where g is the term without SU(3) breaking (three-gluon intermediate state, for instance), h is the SU(3)-violating amplitude due to s quark mass, e is the electromagnetic contribution, and x is the ratio of u- to s-quark masses taken equal to 0.62 (Ref. 32). This formalism is the same

as the one used to analyze vector + pseudoscalar production.[7] Then,

$$R=\frac{3\Gamma(J/\psi\to\omega f_2(1270))}{\Gamma(J/\psi\to\rho^0 A_2^0+\rho^+ A_2^- +\rho^- A_2^+)}=\left[\frac{p_\omega}{p_\rho}\right]^n$$
$$=1.016^n$$

with $n=1$ for S-wave production and $n=5$ for D-wave production. This relation is very well satisfied since $R=1.03\pm0.1$ (Ref. 23).

Comparison with $J/\psi\to\phi f_2'(1525)$ partial width is not so precise since relative strength of g,h,e are not known. With the reasonable assumption that they are similar to those measured for vector + pseudoscalar decays,[7] one expects

$$0.16\le\frac{3\Gamma(J/\psi\to\phi f_2'(1525))}{\Gamma(J/\psi\to\rho^0 A_2^0+\rho^+ A_2^- +\rho^- A_2^+)}\le0.36$$

(S wave),

$$0.06\le\frac{3\Gamma(J/\psi\to\phi f_2'(1525))}{\Gamma(J/\psi\to\rho^0 A_2^0+\rho^+ A_2^- +\rho^- A_2^+)}\le0.12$$

(D wave),

which is consistent with the measured value: 0.23 ± 0.02 using the value of $\phi f_2'(1525)$ measured assuming interference with the $f_2(1720)$ (Table IV) or 0.14 ± 0.02 without interference.

X. LOOKING FOR $\phi\pi$ EXOTICS PRODUCTION

Chanowitz suggested[33] that the $\phi\pi$ system is a good final state to look for exotic bound states like hybrids. A $J^{PC}=1^{--}$, $I=1$ candidate named $C(1480)$ was recently observed at Serpukhov[34] in the reaction $\pi^- p\to\phi\pi^0 n$ with $M_C=(1480\pm40)$ MeV/c^2 and $\Gamma_C=(130\pm60)$ MeV/c^2.

TABLE IV. Summary of the measured branching ratios.

Final state	B (10^4)
$\phi p\bar{p}$	$0.45\pm0.13\pm0.07$
$\phi\pi^+\pi^-$	$7.8\pm0.3\pm1.2$
ϕK^+K^-	$8.3\pm0.3\pm1.3$
$\phi K^0\bar{K}^0$	$6.3\pm0.7\pm1.6$
ωK^+K^-	$7.4\pm0.7\pm2.3$
$\omega K^0\bar{K}^0$	$12.4\pm2.0\pm3.1$
$\phi(K^*\bar{K}+\text{c.c.})\to\phi K\bar{K}\pi$	$20.7\pm2.4\pm3.0$
$\phi(4\pi^\pm)$	$16.0\pm1.0\pm3.0$
$\phi K_S^0 K^\pm\pi^\mp$	$7.4\pm0.9\pm1.1$
$\phi f_0(975)(f_0\to\pi^+\pi^-)$	$2.4\pm0.2\pm0.4$
$\phi f_2(1270)$	<4.5
$\phi\eta(1440)[\eta(1440)\to K\bar{K}\pi]$	<2.5
$\phi f_2'(1525)(f_2'\to K^+K^-)$	$4.4\pm0.2\pm0.7$[a]
$\omega f_2'(1525)(f_2'\to K^+K^-)$	<1
$\phi X(1700)[X(1700)\to K^+K^-]$	$1.8\pm0.1\pm0.3$[b]
$\omega X(1700)[X(1700)\to K^+K^-]$	$2.0\pm0.6\pm0.3$
$\omega X(1700)[X(1700)\to K^0\bar{K}^0]$	2.8 ± 0.9

[a] 2.8 ± 0.1 without interference.
[b] 3.7 ± 0.15 without interference.

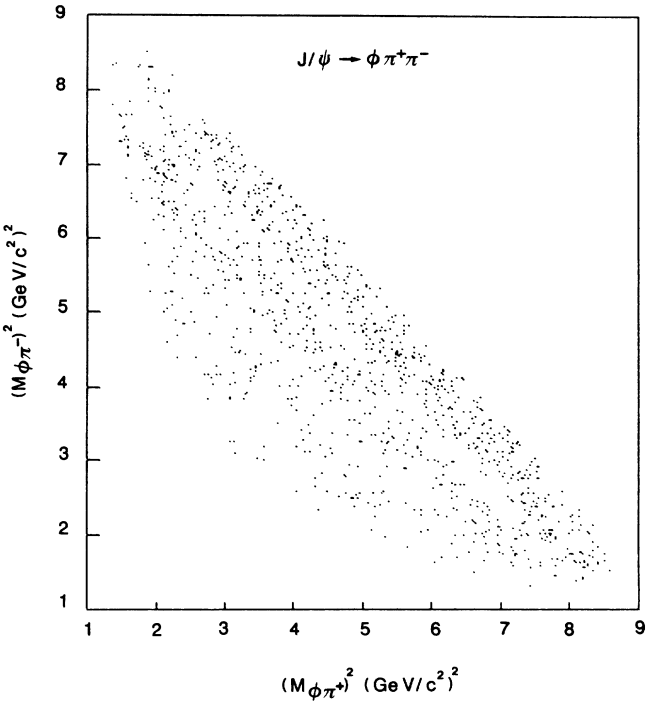

FIG. 34. Dalitz plot of $J/\psi\to\phi\pi^+\pi^-$.

The possibility that this state could be a $q\bar{q}q\bar{q}$ particle has been also investigated.[35]

The hadronic J/ψ decays are a natural place to look for $q\bar{q}g$ states since they involve $q\bar{q}$ and gluons in the intermediate state. Figure 34 shows the Dalitz plot for the $J/\psi\to\phi\pi^+\pi^-$ decay. No $\phi\pi$ structures are evident. Figure 35 shows the $\phi\pi^\pm$ mass spectrum of these events and the expected distribution assuming that the $J/\psi\to\phi\pi^+\pi^-$ decay is dominated by the $J/\psi\to\phi X$, $X(\to\pi^+\pi^-)$ process. It is in good agreement with the data, although an excess of events is still present around 1.5 GeV/c^2 with mass and width consistent with the $C(1480)$ parameters. But the statistical significance of

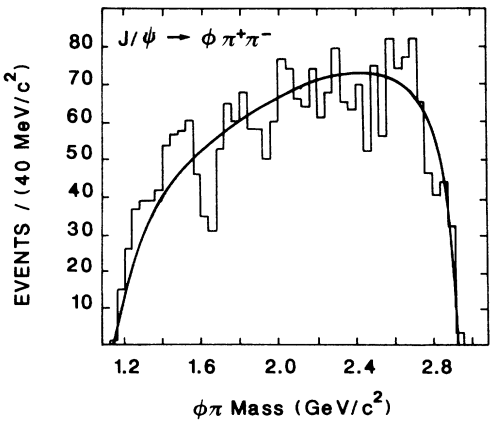

FIG. 35. $\phi\pi^\pm$ distribution in $J/\psi\to\phi\pi^+\pi^-$. The curve is the shape expected by assuming that the $J/\psi\to\phi\pi^+\pi^-$ decay only proceeds through $J/\psi\to\phi X(X\to\pi^+\pi^-)$.

this contribution is too small to claim the existence of the $J/\psi \to C(1480)\pi$ decay and only an upper limit is given:

$$B(J/\psi \to C^{\pm}(1480)\pi^{\mp})B(C^{\pm}(1480) \to \phi\pi^{\pm}) \leq 1.5 \times 10^{-4} \quad (95\%\ \text{C.L.}) .$$

XI. SUMMARY AND CONCLUSIONS

Table IV summarizes the branching-ratio measurements presented in this paper. Values are consistent and strongly improve the results from previous experiments.[8] Although representing a small fraction of all J/ψ decays (less than 1%), the final states studied in this paper exhibit a lot of interesting features.

(i) The nonresonant $\pi\pi$ production associated with the ϕ is small [Fig. 27(b)] as expected from the dominance of connected diagrams which cannot form directly a $\pi\pi$ system from $s\bar{s}$. Surprisingly, this result is also true for the OZI-allowed $K\bar{K}$ production in $J/\psi \to \phi K\bar{K}$ [Fig. 27(c)], whereas the $K^*\bar{K}$ system is quite strongly produced with a phase-space-like dynamics [Fig. 17(c)].

(ii) $f_0(975)$ is produced with a large branching ratio and cannot be correctly fitted by a classical Flatté distribution. A satisfactory analysis with coupled $(\pi\pi, K\bar{K})$ channels was performed, including our present knowledge of low-energy $\pi\pi$ physics.[18] Our data do not reject an exotic structure ($q^2\bar{q}^2, K\bar{K}$ molecule). No additional narrow object is observed below 1 GeV/c^2.

(iii) No definite result can be given for a possible $f_0(1300)$ or $f_2(1270)$ production in $J/\psi \to \phi\pi^+\pi^-$ even though a large activity is observed between 1.1 and 1.5 GeV/c^2.

(iv) No $\eta(1440)$ contribution is observed associated with ϕ. This indicates that this particle does not contain a large $s\bar{s}$ component.

(v) A possible contribution of $J/\psi \to C^{\pm}(1480)\pi^{\mp} \to \phi\pi^+\pi^-$ is consistent with our data, although no significant conclusion can be drawn.

(vi) As expected $f_2'(1525)$, strongly associated with ϕ, remains unobserved associated to ω. This is a clear indication for dominance of connected diagrams [Fig. 2(a)]. The branching ratio of $J/\psi \to \phi f_2'(1525)$ is found in good agreement with the value predicted from SU(3) symmetry and $J/\psi \to \omega f_2(1270)$, ρA_2 branching ratios.

(vii) A state is observed in the decay $J/\psi \to \omega K^+K^-$ with mass and width fully consistent with the $f_2(1720)$ parameters. This is a strong indication for $\omega f_2(1720)$ associated production. An unambiguous identification of the observed state with the $f_2(1720)$ by a spin analysis has not been achieved, due to the small statistics available to reliably measure five independent amplitudes with different momentum dependence. The $\phi f_2(1720)$ production is more controversial. The shoulder observed in the K^+K^- mass spectrum is explained as being produced by the $f_2(1720)$ by assuming an interference between $f_2(1720)$ and $f_2'(1525)$ amplitudes.

ACKNOWLEDGMENTS

We are very indebted to G. Mennessier for useful discussions and for providing us the improved method to describe the $f_0(975)$ production. We acknowledge T. Barnes for interesting comments. We greatly appreciate the efforts of the technical staff of the LAL for the construction and maintenance of the apparatus and the constant support, especially those of the DCI storage rings directed by P. Marin.

[1] D. L. Burke *et al.*, Phys. Rev. Lett. **49**, 632 (1982); R. M. Baltrusaitis *et al.*, *ibid.* **55**, 1723 (1985); R. M. Baltrusaitis *et al.*, Phys. Rev. D **33**, 1222 (1986); D. Bisello *et al.*, Phys. Lett. B **179**, 294 (1986); D. Bisello *et al.*, *ibid.* **192**, 239 (1987); L. Stanco, in *Heavy Flavors,* proceedings, San Miniato, Italy, 1987, edited by F. L. Navarria [Nucl. Phys. B, Proc. Suppl. **1B** (1987)].

[2] B. Jean-Marie, in *Proceedings of the 23rd International Conference on High Energy Physics,* Berkeley, California, 1986, edited by S. C. Loken (World Scientific, Singapore, 1987).

[3] K. Konigsmann, Phys. Rep. **139**, 243 (1986); F. L. Gilman and R. Kauffman, Phys. Rev. D **36**, 2761 (1987).

[4] See, for instance, F. E. Close, *An Introduction to Quarks and Partons* (Academic, New York, 1979).

[5] G. Karl and San-Fu Tuan, Phys. Rev. D **34**, 1629 (1986); G. Karl and W. Roberts, Phys. Lett. **144B**, 263 (1984).

[6] S. S. Pinsky, Phys. Rev. D **31**, 1753 (1985).

[7] A. Seiden *et al.*, University of California, Santa Cruz Report No. SCIPP Report No. 87/73, 1987 (unpublished); A. Falvard, in *Proceedings of the European Physical Society High Energy Physics Conference [International Europhysics Conference on High Energy Physics],* Uppsala, Sweden, 1987, edited by O. Botner (European Physical Society, Geneva, Switzerland, 1987).

[8] M. Aguilar-Benitez *et al.*, Phys. Lett. **170B**, 1 (1986). Some values of the branching ratios given in this reference have to be corrected for relevant Clebsch-Gordan coefficients.

[9] S. R. Sharpe, R. L. Jaffe, and M. R. Pennington, Phys. Rev. D **30**, 1013 (1984).

[10] K. L. Au, D. Morgan, and M. R. Pennington, Phys. Rev. **167**, B229 (1986).

[11] J. E. Augustin *et al.*, Phys. Scr. **23**, 623 (1971).

[12] Here and in the following, the TOF information for each particle, when available, has to be in agreement with the kinematical hypothesis within 3σ.

[13] For the $J/\psi \to \phi\pi\pi, \phi K\bar{K}, \omega K\bar{K}$ decays, efficiencies are determined by generating a set of narrow resonances covering the available $\pi\pi$ or $K\bar{K}$ phase space. Resonances are assumed to be $J^P = 0^+$ or 2^+ objects according to the dynamics observed at the generated mass. Because of the lack of measurements, all the helicity amplitudes are assumed to be identical.

[14] A. Dekmouche, Thèse de l'Université Clermont II, 1987.

[15] J. J. Becker *et al.*, Phys. Rev. Lett. **59**, 186 (1987).

[16] The observed η signal comes from the $J/\psi \to \phi\eta$ decay and will be discussed in a forthcoming paper.

[17] S. M. Flatté, Phys. Lett. **63B**, 224 (1976).

[18]G. Mennessier, Z. Phys. C **16**, 241 (1983).
[19]H. G. Dosch and D. Gromes, Z. Phys. C **34**, 555 (1987).
[20]J. E. Augustin *et al.*, Orsay Report No. LAL/85-27, 1985 (unpublished).
[21]J. Weinstein and N. Isgur, Phys. Rev. Lett. **48**, 659 (1982); Phys. Rev. D **27**, 588 (1983).
[22]T. Barnes and N. Isgur (private communication). Kinematical factors and production of $\omega f_0(975)$ from $\pi\pi$ final-state interaction in the OZI-allowed process $J/\psi \to \omega\pi\pi$ are neglected to compute the factor 2. Then, it indicates only an order of magnitude.
[23]J. E. Augustin *et al.*, Orsay Report No. LAL 88-05 (unpublished).
[24]H. Becker *et al.*, Nucl. Phys. **B151**, 46 (1979).
[25]For a review, see S. Cooper, in *Proceedings of the International Europhysics Conference on High Energy Physics,* Bari, Italy, 1985, edited by L. Nitti and G. Preparata (Laterza, Bari, 1985).
[26]J. E. Augustin *et al.*, Phys. Rev. Lett. **60**, 2238 (1988).
[27]R. M. Baltrusaitis *et al.*, Phys. Rev. D **35**, 2077 (1987).
[28]I. Cohen, N. Isgur, and H. J. Lipkin, Phys. Rev. Lett. **48**, 1074 (1982).
[29]K. Senba and M. Tanimoto, Phys. Rev. D **26**, 3270 (1982). This question was reexamined in F. Caruso and E. Predazzi, Z. Phys. C **33**, 569 (1987).
[30]The fitted phase is always near 180°. This means that the amplitudes for the $f_2'(1525)$ and the $f_2(1720)$ are relatively real with opposite signs. If $X(1700)$ is $f_2(1720)$ and this particle is a glueball, it should be produced dominantly through the disconnected diagram [Fig. 2(b)]. It is to be noted that the same destructive interference between connected and disconnected diagrams is found in the analysis of the $J/\psi \to$ vector + pseudoscalar (Ref. 7).
[31]J. E. Augustin *et al.*, Z. Phys. C **36**, 369 (1987).
[32]J. L. Rosner, Phys. Rev. D **27**, 1101 (1983).
[33]M. S. Chanowitz, in *Multiparticle Dynamics 1983,* proceedings of the XIV International Symposium, Lake Tahoe, Nevada, edited by P. Yager and J. F. Gunion (World Scientific, Singapore, 1984).
[34]S. I. Bityukov *et al.*, Phys. Lett. B **188**, 383 (1987).
[35]F. E. Close and H. J. Lipkin, Phys. Lett. B **196**, 245 (1987).